HEFAT2010
7th International Conference on Heat Transfer, Fluid Mechanics and Thermodynamics
19-21 July 2010
Antalya, Turkey

REAL-GAS EFFECTS IN SUPERCRITICAL CARBON DIOXIDE GASDYNAMIC NOZZLES

Guardone A.
Dipartimento di Ingegneria Aerospaziale,
Politecnico di Milano,
Milano, 20156,
Italy,
E-mail: alberto.guardone@polimi.it

ABSTRACT

A nozzle design tool for real gases has been devised for investigating the features of gasdynamic nozzles operating with supercritical or close to critical carbon dioxide.

Three exemplary real-gas expansions, originating from a reservoir at a temperature of 400 K and at a pressure of 10, 5 and 1 MPa, respectively, were considered and compared to the corresponding dilute gas case, for which reservoir conditions are 400K and 0.1 MPa. Differently from the well-known ideal-gas results, the nozzle shape depends on the reservoir or total flow conditions and therefore diverse designs are obtained for a given exit Mach number depending on the relative location of the initial state in the volume-pressure thermodynamic plane with respect to the liquid-vapor saturation curve. For flow states close to the liquid-vapor saturation curve and critical point, the nozzle length and height are larger than the corresponding ideal gas designs. Differences are as large as 17% for the divergent length and 18.4% for the nozzle height. More relevant differences are found for the mass flow, which for high pressure exceeds its ideal gas value by two order of magnitudes. This difference is mainly due to the effect of the density, which is increases with increasing reservoir density.

NOMENCLATURE

M	[-]	Mach number
P	[Pa]	Pressure
T	[K]	Temperature
c	[m/s]	Speed of sound
s	[J/kg/K]	Specific entropy per unit mass
h	[J/kg]	Specific enthalpy per unit mass
R	[J/kg/K]	Gas constant
c_v	[J/kg/K]	Specific heat at constant volume
u	[m/s]	Fluid x velocity
v	[m/s]	Fluid y velocity
$\dot{m}$	[kg/s]	Mass flow
L	[m]	Nozzle length
H	[m]	Nozzle height
x	[m]	Nozzle axial coordinate
y	[m]	Local nozzle width

Special characters

ρ	[kg/m^3]	Density
Γ	[-]	Fundamental derivative of gasdynamics
Φ	[-]	Full potential
ϕ	[-]	Perturbation potential

Subscripts

c	Critical point
r	Reservoir state
s	Sonic state
t	Nozzle throat section
d	Design or exit conditions
x,y	Partial derivative with respect to x or y

INTRODUCTION

The scientific interest towards the study of nozzle flows in the vicinity of the liquid-vapor saturation curve is driven by diverse industrial applications. These include transonic and hypersonic wind tunnels operating in the dense gas regime [1,2,3], transportation of high-pressure fuels and chemicals, see [4,5], and the use of super-critical hydrogen to cool the surface of aircraft at hypersonic speeds, see [6]. The industrial application of interest here is related to supersonic nozzle flows of supercritical carbon dioxide (CO_2). For example, nozzles are used in pharmaceutical processes to produce under expanded jets of supercritical carbon dioxide to nucleate pharmaceutical components [7].

The design of processes and machinery operating in the vicinity of the liquid-vapor saturation curve is limited by the availability of suitable analysis and design tools and to the limited knowledge on the gasdynamics of real-gas flows.

Indeed, the vast majority of simulation and design tools relies upon the ideal gas approximation of the fluid properties, an assumption that is clearly violated in the thermodynamic region of interest.

Recently numerous simulation codes, including commercial ones, has been modified to allow for the inclusion of non-ideal thermodynamics. Diverse numerical simulations of non-ideal flows around airfoils or turbine cascades have been carried out using complex thermodynamic models in [8,9,10]. Cinnella and Congedo used automatic design CFD techniques for two-dimensional flows to optimize the shape of airfoils operating in the dense gas regime, as a first step towards the optimization of three-dimensional nozzles and turbine blades [11]. If on the one

side Computational Fluid Dynamics (CFD) codes allow for a detailed investigation of the flow field, on the other side the computational burden due to the non-ideal thermodynamic model is usually too high to allow for the use of these tools in the design phase. However, design tools based on simplified models are still missing and no systematic studies to guide the choice of the proper working fluid and operating conditions have been carried out, yet.

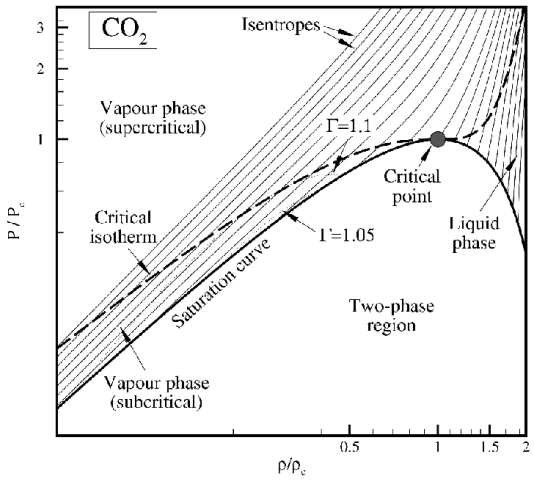

Figure 1 Representative isentropes and liquid-vapor saturation curve in the ρ-P plane for carbon dioxide under the polytropic van der Waals gas. The critical isotherm, the critical point and iso-lines of the fundamental derivative of gasdynamics are also shown.

The present paper reports on preliminary results obtained from a standard design procedure applied to the design of the divergent section of subsonic-supersonic nozzles operated with carbon dioxide in the vapor phase and close to the liquid-vapor saturation curve, see Figure 1. In all figures, reduced variables, made dimensionless by their critical value, are shown. For carbon dioxide, one has T_c = 304.2 K, P_c = 7.3795 MPa, ρ_c = 342.4 kg/m^3.

The design procedure prescribes uniform Mach number M_D and flow velocity parallel to the nozzle axis at the exit section. A standard design technique based on the Method Of Characteristics (MOC) is followed here, in which the simple polytropic (constant isochoric specific heat) van der Waals gas model [12] is used to describe the fluid thermodynamic properties. Although quantitatively very inaccurate, the van der Waals model allows to qualitatively take into account dense gas behavior, including phase change and the non-ideal dependence of the speed of sound on both the temperature and density [13].

NOZZLE DESIGN PROCEDURE

In the present study, two-dimensional nozzles of convergent-divergent type are considered. Nozzles discharge from a reservoir of infinite capacity into an ambient at constant pressure, which is lower or equal to the adapted-flow exit pressure; therefore, the Mach number in the divergent section and at the exit of the nozzle is supersonic. It is assumed here that both the viscous and thermal boundary layer thicknesses are negligible with respect to the nozzle diameter. The effect of the viscosity and of thermal conductivity are therefore neglected in the present study.

Under the above assumptions, the flow is steady and can be described by the well-known potential equation for irrotational compressible flows, namely

$$\left(\Phi_x^2-c^2\right)\Phi_{xx}+2\Phi_x\Phi_y\Phi_{xy}+\left(\Phi_y^2-c^2\right)\Phi_{yy}=0, \qquad (1)$$

where x and y are the Cartesian coordinates, Φ is the velocity potential, where $u = \Phi_x$ and $v = \Phi_y$ are the x and y velocity components, respectively, and where the subscripts indicate partial derivatives [14].

The fluid thermodynamic enters Eq. (1) only through the definition of the speed of sound $c = c(h,s)$, with h specific enthalpy and s specific entropy per unit mass. In the present case of uniform total specific enthalpy and entropy, the speed of sound in Eq. (1) is a function of the velocity module only, via the simple relation

$$c(w)=c\left(h_r-w^2/2, s_r\right) \qquad (2)$$

where w is the velocity module and the subscript r indicate reservoir or stagnation conditions. The evaluation of the sound speed function (2) requires one to specify a complete thermodynamic model of the fluid. This task can be accomplished for example by providing the two (compatible) equations of state for the pressure P and the internal energy per unit mass e as functions of the temperature T and the density ρ. For the polytropic van der Waals gas of interest here these reads

$$P(T,\rho)=\frac{RT\rho}{1-b\rho} \qquad e(T,\rho)=c_v T-a\rho \qquad (3)$$

where R is the specific gas constant, a is a gas-dependent parameter related to long range attractive intermolecular forces, b is related to short range repulsive ones and c_v is the isochoric specific heat. For carbon dioxide, the constant value of the isochoric specific heat reads $c_v / R = 3.5$.

The design procedure of the divergent section of the nozzle moves from the determination of the transonic flow at the nozzle throat. The transonic flow region is described by the well known equation for the perturbation potential ϕ,

$$2\Gamma_s\varphi_x\varphi_{xx}-\varphi_{yy}=0 \qquad (4)$$

for non-ideal thermodynamic model [15,16,17]. In Eq. (4), the subscript s indicate sonic condition and

$$\Gamma=1+\frac{\rho}{c}\left(\frac{\partial c}{\partial \rho}\right)_s \qquad (5)$$

is the fundamental derivative of gasdynamics. The value of the fundamental derivative is of paramount importance for the determination of the gasdynamic behavior of the fluid [18]. It assumes the constant value Γ = (γ + 1) / 2 for a polytropic ideal gas model, with γ specific heats ratio.

The transonic potential equation (4) is solved by means of the approximate solution procedure of Sauer [19], which is applicable to real-gas flow without significant modifications. The transonic flow solution provides the initial data curve for the Method of Characteristics, which has been implemented in the present work according to the textbook of Zucrow and Hoffman [14]. The expansion in the divergent section to the desired design Mach number M_D is achieved via an initial circular profile followed by the so-called turning region, in which the nozzle upper wall geometry is determined by imposing the conservation of the mass flow at each section. The resulting flow at the nozzle exit is with uniform Mach number M_D and parallel to the x axis. Further details on the design procedure can be found in [14].

NOZZLE DESIGN FOR REAL GASES

The nozzle design procedure described in the previous section is now applied to the design of subsonic-supersonic nozzles operating with carbon dioxide and in the vicinity of the critical isotherm.

Recovery of dilute gas results

As a preliminary step and to verify the correctness of the numerical results, ideal gas computations are compared against data available in the literature and the behavior of van der Waals model in the dilute gas limit is verified.

The reference case is that presented in [14], where a polytropic ideal gas model of molecular Nitrogen is used to design the divergent section of a subsonic-supersonic nozzle. In all computations, $c_v / R = 2.564$ for Nitrogen and $M_d = 3$.

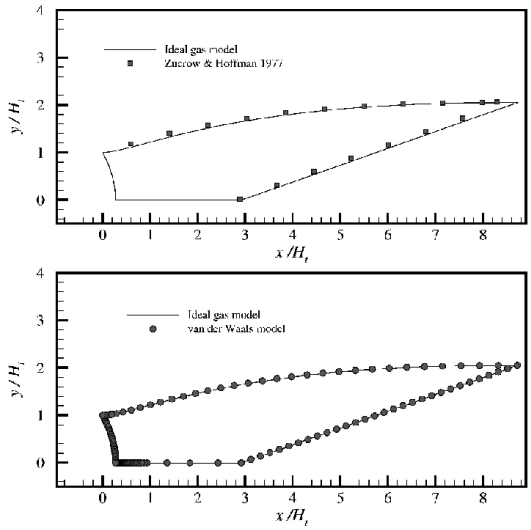

Figure 2 Comparison of a reference nozzle design obtained using the ideal gas model against reference data [14] for molecular Nitrogen (top) and comparison of ideal gas design with the van der Waals gas model in dilute conditions (bottom). In both cases $M_d = 3$.

Figure 2 (top) shows the design obtained by using the present approach under the polytropic ideal gas model. Results compare fairly well with those presented by Zucrow and Hoffman [14]. The consistency of the van der Waals model in the dilute limit is verified by comparisons in Figure 2 (bottom), where as expected both the ideal gas model and the van der Waals model are shown to compute the same geometries in dilute gas conditions.

Numerical convergence with respect of the number of initial data points is checked in all computations against the mass flow value at each characteristic fronts. Thanks to the very low computational cost of the design procedure, as many as 101 initial characteristic nodes are used in all computations, which results in a total number of characteristic nodes of about 20 000. With this relatively fine computational net, the relative error for the mass flow at each node is lower than 10^{-4} for all computations.

Nozzle design for supercritical and close to critical CO_2

In the present section, four selected expansion conditions are examined. In all cases, the flow expands from a reservoir at constant conditions, where the fluid is assumed to be at rest, to an uniform flow parallel to the x axis at the exit, with exit Mach number $M_d = 3$.

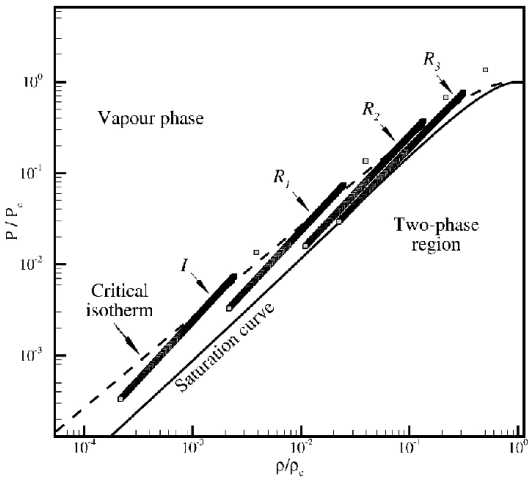

Figure 3 Thermodynamic states for the ideal and real gas study cases in the ρ-P thermodynamic plane. All flow states occurring inside the nozzle are plotted as square symbols.

In Figure 3, the thermodynamic states within the divergent section are plotted in the density-pressure plane for all cases. Study cases are chosen so to investigate real-gas effects in the single-phase vapor region and are labeled as case I for ideal, which is taken as the reference case, and R_1, R_2, R_3, with increasing real-gas effects.

Reservoir conditions are listed for all cases in Table 1, where the reservoir temperature, pressure, density, fundamental derivative and compressibility are listed. In Table 2, sonic conditions for each case are reported, including the value of the fluid velocity which is coincident with the local value of the speed of sound. In Table 3, exit conditions are reported. The reservoir temperature is 400 K, or $T_r / T_c = 1.31$, for all cases. Reservoir states are all within the vapor phase.

Note that the local value of the fundamental derivative of gasdynamics Γ and the compressibility factor $Z = P/(RT\rho)$ indicate departure from ideal gas conditions. Indeed, the polytropic ideal gas model of CO_2 gives $\Gamma_{ideal} = (\gamma + 1) / 2 = 1.143$ and of course $Z_{ideal} = 1$.

Case	T_r [K]	P_r [MPa]	ρ_r [kg/m³]	Γ_r	Z_r
I	400.0	0.100	1.326	1.142	0.998
R_1	400.0	1.000	13.51	1.140	0.980
R_2	400.0	5.000	74.13	1.143	0.893
R_3	400.0	10.00	171.4	1.261	0.772

Table 1 Reservoir thermodynamic conditions for the ideal and real gas study cases.

Case	T_s [K]	P_s [MPa]	ρ_s [kg/m³]	Γ_s	Z_s	$u_s = c_s$ [m/s]
I	349.9	0.055	0.831	1.142	0.998	291.2
R_1	349.4	0.550	8.459	1.139	0.984	288.3
R_2	346.9	2.774	46.33	1.126	0.914	273.7
R_3	343.4	5.623	107.9	1.134	0.800	251.7

Table 2 Thermodynamic states at sonic conditions for the ideal and real gas study cases.

Case	T_d [K]	P_d [MPa]	ρ_d [kg/m³]	Γ_d	Z_d	u_d [m/s]
I	174.9	0.0024	0.073	1.143	1.000	618.1
R_1	173.5	0.0240	0.736	1.141	0.996	614.3
R_2	166.9	0.1155	3.733	1.134	0.981	595.6
R_3	156.2	0.2148	7.594	1.123	0.959	566.3

Table 3 Thermodynamic states at the nozzle exit for the ideal and real gas study cases for $M_d = 3$.

In case I, the expansion process is sufficiently far from saturation to be considered as ideal, a result confirmed by the value of Γ and Z in the reservoir, at sonic condition and at the exit of the nozzle. In cases R_1 , Γ and Z slightly depart from ideal gas values; in case R_2 and R_3 the expansion process ends very close to the liquid-vapor saturation curve and real gas effects are more evident.

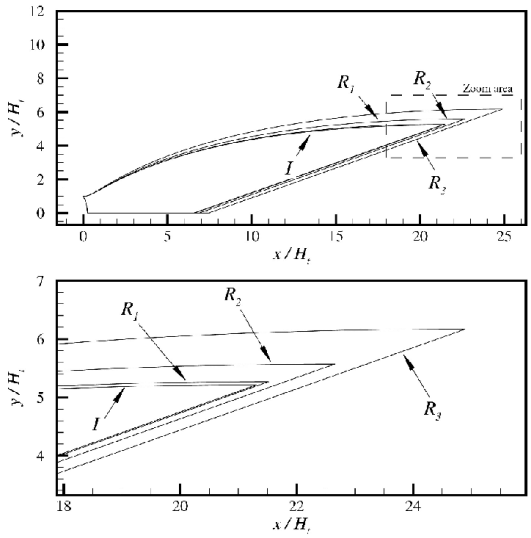

Figure 4 Nozzle geometries for the ideal and real gas study cases for $M_d = 3$ (top). Details of the exit section (bottom).

In Figure 4, the nozzle geometries obtained by the design procedure are plotted. For expansion processes that occur close to the saturation curve, the nozzle length L and height H are larger than the corresponding ideal gas cases. Moreover, nozzle dimensions monotonically increase with the reservoir pressure, that is, with the degree of gas non-ideality.

Case	L_d / H_t	H_d / H_t	$\dot{m} / H_t$ [kg/(m s)]	$\Delta L_{IR}/H_t$	$\Delta H_{IR}/H_t$	$\Delta\dot{m}/H_t$
I	21.31	5.21	241.99	-	-	-
R_1	21.52	5.27	2438.4	1.0%	1.1%	908%
R_2	22.66	5.57	12679	6.0%	6.9%	5140%
R_3	24.90	6.17	27167	17.0%	18.4%	11126%

Table 4 Nozzle length, height and mass flow for the ideal and real gas study cases for $M_d = 3$. Relative differences are also shown

Relevant results for the considered designs are reported in Table 4, where the nozzle length, height and the mass flow per unit length are reported. The reference length is the nozzle height at the throat section H_t. For comparison, relative differences with respect to the ideal gas are also shown. These are defined as $\Delta L_{IR} = (L_{d,\,real} - L_{d,\,ideal}) / L_{d,\,ideal}$, $\Delta H_{IR} = (H_{d,\,real} - H_{d,\,ideal}) / H_{d,\,ideal}$ and $\Delta\dot{m} = (\dot{m}_{d,\,real} - \dot{m}_{d,\,ideal}) / \dot{m}_{d,\,ideal}$. The design procedure in the real gas case R_3 gives a nozzle that is 17% longer and 18.4% higher than the corresponding ideal gas design at the exit section.

The above results on the nozzle dimensions are consistent with the simple quasi-one-dimensional model of nozzle flows for real gases which gives the well-known relation [19]

$$\frac{dM}{dA} = -\frac{1+(\Gamma-1)M^2}{1-M^2}\frac{M}{A} \qquad (6)$$

where A is the nozzle cross-sectional area, which corresponds to the y coordinate of the nozzle upper wall in the present two-dimensional approximation. Indeed, for all considered design conditions, the expansion process crosses a thermodynamic region in which the fundamental derivative of gasdynamics Γ is always lower than the corresponding polytropic ideal gas value, which for carbon dioxide is $\Gamma_{ideal} = (\gamma+1) / 2 = 1.143$, to be confronted with the Γ iso-lines for carbon dioxide under the polytropic van der Waals approximation shown in Figure 1. Therefore, at a given Mach number M, the value of dM/dA in the real-gas region is always lower than that obtained from the polytropic ideal gas model and the final exit area A_d, that is y_d in the present case, is always larger in the real-gas cases. Correspondingly, since the slope of the last characteristic line is the same for all considered cases, for which one always has $M_d = 3$, real-gas conditions result also in longer nozzle designs with respect to the ideal gas case.

The most relevant differences with respect to the ideal gas cases are found for the mass flow per unit length, see Table 4. Indeed, the mass flow for the real gas case R_3 is two order of magnitude larger than that in the ideal gas case. These large differences are not surprising due to the diverse thermodynamic conditions at which the expansion process occurs. It is remarkable that differences in the mass flow per unit length are found to be mainly related to the differences in value of the fluid density at sonic states or at the nozzle exit, since the local flow velocity does not change significantly for the diverse study cases. Note that the fluid velocity in these conditions is in a one to one correspondence to the local value of the speed of sound, since one has $u_s = c_s$ at sonic

condition and $u_d = M_d\, c_d$ at the exit section. Despite the relative non-ideality of the thermodynamic conditions of the process, the speed of sound is found to depend only slightly on the value of the pressure and to depend mainly on that of the fluid temperature, which is almost the same for all cases. Therefore, one can conclude that the nozzle volume flow rate, which is relevant to many industrial applications, is almost the same for all considered cases.

CONCLUSION

A standard nozzle design procedure was applied to the design of the divergent section of two-dimensional convergent-divergent nozzles operating in adapted-flow conditions. A small-perturbations solution of the transonic flow at the nozzle throat has been used to provided the initial data to the method of characteristics, which has been generalized to the polytropic van der Waals fluid model. As it is standard practice, the design of the supersonic divergent section is carried out by imposing uniform flow condition at the nozzle exit section, with velocity parallel to the nozzle axis. The expander geometry is then computed by enforcing the conservation of the mass flow at each cross section. The design procedure was generalized to the well-known van der Waals gas model to investigate the effects of non-ideal gas behavior on the nozzle design of carbon dioxide expanders in the supercritical and close-to-critical thermodynamic region.

Three exemplary real-gas expansions, originating from a reservoir at a temperature of 400 K and at a pressure of 10, 5 and 1 MPa, respectively, were considered and compared to the corresponding dilute gas case, for which reservoir conditions are 400K and 0.1 MPa.

The nozzle geometry is found to be significantly influenced by real-gas effects. In particular, for flow states close to the liquid-vapor saturation curve and critical point, the nozzle length and height are larger than the corresponding ideal gas designs. Differences are as large as 17% for the divergent length and 18.4% for the nozzle height. More relevant differences are found for the mass flow, which for high pressure exceeds its ideal gas value by two order of magnitudes. This difference is mainly due to the effect of the density, which is increases with increasing reservoir density.

As a final remark, a commentary on the validity and limitations of the presented results is given. First, the design discussed in the present work are so-called inviscid designs, namely, the geometry is to be corrected to account for the presence of a viscous boundary layer, provided that the latter does not detach from the nozzle walls. Secondly, the simple van der Waals gas model is known to provide a good qualitative description of close-to-saturation vapors but to be fairly inaccurate. A quantitative evaluation of the influence of non-ideal effects in the nozzle design requires therefore to consider more complex thermodynamic descriptions of the fluid. Finally, the thermodynamic region that is investigated in the present work is very limited and far from being representative of all real-gas effects. Research activities are currently under-way to study the complete real gas thermodynamic region and to investigate the behavior of different types of fluids.

ACKNOWLEDGMENTS

The help of Vincent Vandecauter in the development of the computer code is acknowledged.

REFERENCES

[1] Enkenhus, K. R. & Parazzoli, C. 1970 Dense gas phenomenon in a free-piston hypersonic wind tunnel. AIAA J. 8, 60–65.Anders, J. B. 1993 Heavy gas wind-tunnel research at Langley Research Center. In Fluid Engineering Conference, June 20-24, Washington, DC. ASME Paper 93-FE-5.

[2] Wagner, B. & Schmidt, W. 1978 Theoretical investigation of real gas effects in cryogenic wind tunnels. AIAA J. 16, 580–586.

[3] Anderson, W. K. 1991 Numerical study on using sulfur hexafluoride as a test gas in wind tunnels. AIAA J. 29, 2179–2180.

[4] Bobe, W. & Chow, W. L. 1990 Nonideal isentropic gas flow through converging-diverging nozzles. ASME J. Fluids Eng. 112, 455–460.

[5] Leung, J. C. & Epstein, M. 1988 A generalized critical model for nonideal gases. AIChE J. 34, 1568–1572.

[6] Dziedzidzic, W. M., Jones, S. C., Gould, D. C. & Petley, D. H. 1993 Analytical comparison of convective heat transfer correlation in supercritical hydrogen. J. Thermophys. Heat Tr. 7 (1), 68–73.

[7] Subramaniam, B., Rajewski, R. A. & Snavely, K. 1997 Pharmaceutical processing with supercritical carbon dioxide. J. Pharm. Sci. 86 (8), 885–890.

[8] Hoffren, J., Talonpoika, T., Larjola, J., and Siikonen, T., 2002, "Numerical Simulation of Real-Gas Flow in a Supersonic Turbine Nozzle Ring," ASME J. Eng. Gas Turbines Power, 1242, pp. 395–403.

[9] Cinnella, P. & Congedo, P. M. 2007 Inviscid and viscous aerodynamics of dense gases. J. Fluid Mech. 580, 179–217.

[10] Colonna, P., Harinck, J., Rebay, S. & Guardone, A. 2008 Real-gas effects in Organic Rankine Cycle turbine nozzles. J. Propul. Power 24 (2), 282–294.

[11] Cinnella, P. & Congedo, P. M. 2008 Optimal airfoil shapes for viscous transonic flows of Bethe–Zeldovich–Thompson fluids. Comput. & Fluids 37, 250–264.

[12] van der Waals, J. D. 1988 On the continuity of the gaseous and liquid states, , vol. XIV. North-Holland, reprinted.

[13] Colonna, P. & Guardone, A. 2006 Molecular interpretation of nonclassical gasdynamics of dense vapors under the van der Waals model. Phys. Fluids 18 (5), 056101–1–14.

[14] Zucrow, M. H. & Hoffman, J. D. 1977 Gas dynamics: multidimensional flow, , vol. 2. Wiley, Jhon & Son.

[15] Schnerr, G. H. & Molokov, S. 1994 Exact solutions for transonic flows of dense gases in two-dimensional and axisymmetric nozzles. Phys. Fluids 6 (10), 3465–3471.

[16] Schnerr, G. H. & Molokov, S. 1995 Nonclassical effects in two-dimensional transonic flows. Phys. Fluids 7 (11), 2867–2875.

[17] Rusak, Z. & Wang, C. 1997 Transonic flow of dense gases around an airfoil with parabolic nose. J. Fluid Mech. 346, 1–21.

[18] Thompson, P. A. 1971 A fundamental derivative in gas dynamics. Phys. Fluids 14 (9), 1843–1849.

[19] Sauer, R. 1947 General characteristics of the flow through nozzles at near critical speeds. TM 1147. NACA.